



Published in final edited form as:

Langmuir. 2011 August 2; 27(15): 9597–9601. doi:10.1021/la201801e.

Antibacterial Fluorinated Silica Colloid Superhydrophobic Surfaces

Benjamin J. Privett^a, Jonghae Youn^b, Sung A Hong^b, Jiyeon Lee^b, Junhee Han^b, Jae Ho Shin^b, and Mark H. Schoenfish^a

Mark H. Schoenfish: schoenfish@unc.edu

^aDepartment of Chemistry, University of North Carolina at Chapel Hill, CB 3290, Chapel Hill, NC 27599, USA

^bDepartment of Chemistry, Kwangwoon University, Seoul, Korea

Abstract

A superhydrophobic xerogel coating synthesized from a mixture of nanostructured fluorinated silica colloids, fluoroalkoxysilane, and a backbone silane is reported. The resulting fluorinated surface was characterized using contact angle goniometry, SEM, and AFM. Quantitative bacterial adhesion studies performed using a parallel plate flow cell demonstrated that the adhesion of *Staphylococcus aureus* and *Pseudomonas aeruginosa* were reduced by 2.08 ± 0.25 and 1.76 ± 0.12 log over controls, respectively. This simple superhydrophobic coating synthesis may be applied to any surface regardless of geometry and does not require harsh synthesis or processing conditions, making it an ideal candidate as a biopassivation strategy.

Introduction

The development of non-fouling coatings remains an important objective for the next generation of marine hulls, optical surfaces, and medical devices. Indeed, microbial fouling of biomedical devices (i.e., catheters, artificial joints) often results in blood stream infections (BSI) that have long plagued the healthcare industry. In 2002, 17 million cases of hospital acquired infections were reported in the United States resulting in roughly 100,000 deaths and \$45 billion in direct medical costs.^{1, 2} The increasing prevalence of these devices and the concomitant rise in associated infections have led to widespread dissemination of antibiotics, resulting in the emergence and rapid spread of drug-resistant microbes.³

As such, the development of device coatings capable of resisting microbial colonization has become a major thrust of research with recent activity focusing on the active release of antibiotics⁴ or broad-spectrum antimicrobials such as silver ions or nitric oxide.^{5, 6} To date, concerns about toxicity,⁷ microbial resistance,^{3, 8} and finite release lifetime⁹ have limited the use and effectiveness of such coatings. Passive strategies including the physical or chemical modification of surfaces have been developed to resist bacterial adhesion in the absence of antimicrobial release, although such approaches have been pursued for decades with limited success.¹ For example, polymers including polyurethane¹⁰ and poly(ethylene glycol) have been shown to reduce in vitro bacterial adhesion,¹¹ but their in vivo effectiveness varies widely with surface chemistry, polymer composition and bacterial species.

Ideal non-fouling coatings not only resist adhesion of fouling agents (i.e., microorganisms), but allow for easy removal of contamination that may occur. Examples of “self-cleaning” surfaces that exist in nature include lotus leaves and water strider legs. These surfaces are referred to as “superhydrophobic,” and exhibit static water contact angles $>150^\circ$.^{12, 13} The preparation of synthetic superhydrophobic surfaces generally involves surface modification via nanoparticles, photolithography, mesoporous polymers or surface etching resulting in nanoscale surface roughness, sometimes in conjunction with additional chemical modifications to reduce surface energy.^{12, 14–16} The latter often require harsh synthetic conditions (e.g., etching and high temperature)^{17, 18} and complex fabrication techniques,^{19, 20} thus limiting the substrate type and geometry that may be coated.^{18, 19, 21} While previous reports have highlighted the utility of superhydrophobic surfaces for reducing fouling, few have evaluated the ability of such surfaces to resist the adhesion of medically-relevant bacteria.^{22–24} Of those evaluations published, assays were non-quantitative^{22, 24} or did not evaluate the viability of attached bacteria.²³ Herein, we describe the synthesis of a superhydrophobic fluoroalkoxysilane coating that unlike previous reports makes use of mild reaction and curing conditions, and should enable modification of any substrates regardless of size or geometry. Using a quantitative bacterial adhesion/viability assay, we demonstrate the utility of this coating to reduce bacterial adhesion.

Experimental Details

Silica colloids were synthesized by sonicating a mixture of (heptadecafluoro-1,1,2,2-tetrahydrodecyl)trimethoxysilane (17FTMS) and tetraethylorthosilicate (TEOS) for 5 min. The amount of 17FTMS in the silane mixture was varied between 0 and 70 mol% (6.23 mmol total silane). The silane mixture was then added dropwise to a stirred solution of 30 mL ethanol (absolute) and 12 mL ammonium hydroxide (28%, w:w) over 30 min to form silica colloids. After an additional 20 min of mixing at room temperature, a white precipitate was collected via centrifugation at $4500 \times g$, washed twice with ethanol, and dried overnight under ambient conditions.

Silica colloid-doped 17FTMS/methyltrimethoxysilane (MTMOS) films were prepared via dispersing 400 mg silica colloids in 9.4 mL cold ethanol via sonication, and then adding 17FTMS and MTMOS. The amount of 17FTMS in the silane mixture was varied between 0 and 40 mol% (1 mmol total silane). Following 5 min of additional sonication, the mixture was added to a flask containing 2 mL H₂O and 200 μ L 0.1 M HCl and stirred for 1 h. The sol solution was spread-cast onto ozone/UV-treated glass slides (69.4 μ L sol solution per cm²) and dried overnight, resulting in an opaque white film or xerogel. The control sols without colloids were spincoated onto 9×24 mm glass substrates (200 μ L at 3000 rpm for 10 s) as simple spread-casting resulted in non-uniform coatings.

The wettability of the resulting surfaces was characterized via static water contact angle goniometry. Reported results are an average of 12 measurements. Surface morphology was characterized via electron microscopy after coating with 2.5 nm Au/Pd and imaging using a Hitachi S-4700 scanning electron microscope. Root-mean-square (RMS) roughness of the substrates was measured via atomic force microscopy, and were calculated from 20 μ m² images of three different substrates obtained in AC mode in air using an Asylum MFP-3D AFM and Olympus AC240TS silicon beam cantilevers (spring constant of 2 Nm⁻¹). MFP-3D software was used for calculation of RMS values. The stability of the coatings was assessed via daily contact angle measurements while soaking the substrates in water at 25 °C for 15 d.

Bacterial adhesion to the substrates was characterized using a parallel-plate flow cell. *S. aureus* and *P. aeruginosa* were grown overnight from a frozen (-80°C) stock in tryptic soy

broth (TSB) at 37 °C, reinoculated in fresh TSB (37 °C), and grown to 10^8 colony forming units (CFU)/mL as determined by optical density at 600 nm and verified by replicate plating on nutrient agar. The bacteria were pelleted via centrifugation ($4500 \times g$, 15 min) and resuspended in an equivalent volume of PBS. The bacterial suspension was flowed over the xerogel substrates at 0.2 mL/min in a custom-machined polycarbonate parallel-plate flow cell (chamber dimensions = $2.1 \times 0.6 \times 0.08 \text{ cm}^3$) for 90 min. The bacterial suspension was then exchanged with sterile PBS without passage of an air-water interface and flowed for another 20 min to rinse away any non-adherent bacteria. The substrates were removed, immersed in 5 mL sterile PBS, and subjected to ultrasonication for 15 min to remove adhered bacteria from the substrates. Bacterial suspensions were then serially diluted, plated on tryptic soy agar, and enumerated after incubation at 37 °C for 24 h.

Results and Discussion

Silica colloids were synthesized from 17FTMS (0 – 70 mol% total silane) and TEOS via base-catalyzed hydrolysis and condensation. The resulting silica colloids were composed of agglomerated silica particles with both micro-scale particle agglomerates (Figure 1A) and nano-scale individual particle definition (Figure 1B).

Xerogel coatings with and without added colloids were synthesized from 17FTMS (0 – 40 mol% total silane) and MTMOS via acid-catalyzed hydrolysis and condensation. The xerogel served as a low surface energy chemical modification to hold the silica colloids in place. Control surfaces consisted of 1) 17FTMS colloids without the additional 17FTMS xerogel coating (i.e., 100 mol% MTMOS); 2) 30 mol% 17FTMS/MTMOS xerogel coating without colloids; and, 3) a 100 mol% MTMOS xerogel coating without colloids. Contact angle goniometry (CAG) was used to measure static water contact angles of the control and silica colloid-doped xerogels. As shown in Figure 2, the optimal 17FTMS concentrations for both silica colloids alone and the xerogel blanks (without doped silica colloids) was 20–30 mol%. Increasing the 17FTMS concentration above 30 mol% 17FTMS did not significantly increase the water contact angles, but negatively impacted the quality of the resulting films (data not shown).

Thus, 30 mol% 17FTMS was used for all fluorinated colloid and xerogel film compositions. Static water contact angle images of the silica colloid-modified xerogels (superhydrophobic films) and controls, and blanks are shown in Table 1. Doping the silica colloids into 17FTMS xerogels resulted in a superhydrophobic interface that was not achievable with silica colloids or 17FTMS xerogels alone.

Scanning electron microscopy (SEM) images of the resulting silica colloid-containing fluorinated xerogel surfaces revealed a dense assembly of agglomerated particles consisting of both micro- and nano-scale features (Figure 3), which are prerequisite surface properties for obtaining superhydrophobicity.¹²

The 17FTMS/MTMOS xerogel film was not apparent in the SEM images as it was spread as a thin coating on the high surface area created by the colloids. Both fluorinated and non-fluorinated blank substrates (without colloids) were characterized with a slight surface roughness of 11.7 ± 0.3 and 1.5 ± 1.3 nm, respectively. As expected, the surface roughness of the 17FTMS colloid-doped substrates was much greater (898.5 ± 84.8 and 573.8 ± 154 nm for fluorinated and non-fluorinated xerogels, respectively). The substantially greater surface roughness for the silica colloid-containing fluorinated substrates may be attributed to the assembly of the hydrophobic silica colloids within the hydrophobic 17FTMS. Indeed, comparison of scanning electron micrographs of both fluorinated and non-fluorinated

colloid doped substrates revealed flat islands of colloids on non-fluorinated surfaces but no such features on the fluorinated interface (Figure 4).

The presence of the smoother colloid islands would be expected to reduce both the measured surface roughness and resulting superhydrophobic character of the films. The stability of the coatings was evaluated by soaking substrates in distilled water for 15 days while measuring the static water contact angle each day. Contact angles were maintained for all four substrates over this period (Figure 5), indicating that these xerogel-modified interfaces are sufficiently stable in aqueous solutions.

Furthermore, the static water contact angle for the fluorinated superhydrophobic substrate ($\sim 167^\circ$) remained constant under the conditions of the bacteria experiment (25°C in phosphate buffered saline) over the course of the bacterial adhesion assay.

Bacterial infection of pin tracts represents the most common complication associated with external fixation of orthopedic biomaterials.^{25–27} We thus evaluated the adhesion of Gram-positive *Staphylococcus aureus* and Gram-negative *Pseudomonas aeruginosa*, strains common to pin tract infections, to control and superhydrophobic surfaces, using a conventional flow cell assay.

As shown in Figure 6, the adhesion of *S. aureus* and *P. aeruginosa* to the silica colloid-doped fluorinated substrates was reduced by 99.0 and 98.2% (2.08 and 1.76 logs, respectively) versus the MTMOS blank. For silica colloid-coated substrates lacking the additional fluorosilane film modification, the reduction in *S. aureus* and *P. aeruginosa* adhesion versus MTMOS was an order of magnitude less at 87.4 (0.93 log) and 91.3% (1.10 log), respectively. Bacterial adhesion to fluorinated and non-fluorinated controls (without colloids) were identical within error as shown at A in Figure 6, indicating that the low surface energy of the fluorinated surface alone does not reduce bacterial adhesion. While these results suggest that the surface roughness of the silica colloid coatings alone may reduce bacterial adhesion, the low surface energy fluorosilane modification further improves the non-fouling nature of the surfaces as observed previously.²⁸ Although the increase in static water contact angle upon fluorine modification was similar ($\sim 16^\circ$), only the colloid-containing substrates showed a measurable decrease in bacterial adhesion (1-log reduction for fluorinated versus non-fluorinated). These results suggest that the greater surface roughness observed for the colloid-containing fluorinated surfaces plays a major role in the observed bacterial adhesion, compared to the 17FTMS coating alone.

Conclusions

The simple and flexible synthesis of silica colloid-based superhydrophobic surfaces has been reported and represents an important advance in developing non-fouling surface coatings. The combination of micro- and nanostructured features from silica colloids and a low surface energy fluorinated silane xerogel resulted in surfaces that reduce the adhesion of highly pathogenic *S. aureus* and *P. aeruginosa* by ~ 2 orders of magnitude vs. controls, making these surfaces excellent candidates for further study as medical device coatings. By utilizing well-defined sol-gel chemistry for colloid and xerogel synthesis, the surface chemistry and physical properties of the resulting coatings may be tuned and optimized depending on the applications. Future studies will focus on the effect of colloid size, surface roughness, backbone silane structure and concentration, and protein preconditioning on bacterial adhesion. Furthermore, the bacterial adhesion of the superhydrophobic surfaces may be further reduced with additional silane precursor modifications that enable the active release of biocidal agents. For example, we have previously reported on silica nanoparticles and xerogels capable of releasing antimicrobial concentrations of nitric oxide.^{5, 29}

Acknowledgments

The authors gratefully acknowledge the U.S. National Institutes of Health (EB000708) and the National Research Foundation of Korea (MEST 2010-0016248) for support of this research. We also thank Katelyn Reighard for assistance with the xerogel surface roughness measurements.

REFERENCES

1. Francolini I, Donelli G. *FEMS Immunol. Med. Microbiol.* 2010; 59:227–238. [PubMed: 20412300]
2. Scott RD. Division of Healthcare Quality Promotion National Center for Preparedness, Detection, and Control of Infectious Diseases Coordinating Center for Infectious Disease Centers for Disease Control and Prevention. 2009 March.
3. Andersson DI, Hughes D. *Nat. Rev. Microbiol.* 2010; 8:260–271. [PubMed: 20208551]
4. Zilberman M, Elsner JJ. *J. Control. Release.* 2008; 130:202–215. [PubMed: 18687500]
5. Hetrick EM, Schoenfisch MH. *Biomaterials.* 2007; 28:1948–1956. [PubMed: 17240444]
6. Kumar R, Munstedt H. *Biomaterials.* 2005; 26:2081–2088. [PubMed: 15576182]
7. Rai M, Yadav A, Gade A. *Biotechnol. Adv.* 2009; 27:76–83. [PubMed: 18854209]
8. Chopra I. *J. Antimicrob. Chemother.* 2007; 59:587–590. [PubMed: 17307768]
9. Hetrick EM, Schoenfisch MH. *Chem. Soc. Rev.* 2006; 35:780–789. [PubMed: 16936926]
10. Dickinson RB, Nagel JA, Proctor RA, Cooper SL. *J. Biomed. Mater. Res.* 1997; 36:152–162. [PubMed: 9261676]
11. Kingshott P, Wei J, Bagge-Ravn D, Gadegaard N, Gram L. *Langmuir.* 2003; 19:6912–6921.
12. Li XM, Reinhoudt D, Crego-Calama M. *Chem. Soc. Rev.* 2007; 36:1350–1368. [PubMed: 17619692]
13. Blossey R. *Nat. Mater.* 2003; 2:301–306. [PubMed: 12728235]
14. Sarkar DK, Saleema N. *Surf. Coat. Tech.* 204:2483–2486.
15. Zhang H, Lamb R, Lewis J. *Science and Technology of Advanced Materials.* 2005; 6:236–239.
16. Wang HX, Fang J, Cheng T, Ding J, Qu LT, Dai LM, Wang XG, Lin T. *Chem. Commun.* 2008:877–879.
17. Fresnais J, Chapel JP, Benyahia L, Poncin-Epaillard F. *J Adhes. Sci. Technol.* 2009; 23:447–467.
18. Hikita M, Tanaka K, Nakamura T, Kajiyama T, Takahara A. *Langmuir.* 2005; 21:7299–7302. [PubMed: 16042457]
19. Yang HT, Jiang P. *Langmuir.* 2010; 26:12598–12604. [PubMed: 20617800]
20. Bravo J, Zhai L, Wu ZZ, Cohen RE, Rubner MF. *Langmuir.* 2007; 23:7293–7298. [PubMed: 17523683]
21. Furstner R, Barthlott W, Neinhuis C, Walzel P. *Langmuir.* 2005; 21:956–961. [PubMed: 15667174]
22. Crick CR, Ismail S, Pratten J, Parkin IP. *Thin Solid Films.* 2011; 519:3722–3727.
23. Fadeeva E, Truong VK, Stiesch M, Chichkov BN, Crawford RJ, Wang J, Ivanova EP. *Langmuir.* 2011; 27:3012–3019.
24. Yonghao X, Hess DW, Wong CP. 2007:1218–1223.
25. Mahan J, Seligson D, Henry SL, Hynes P, Dobbins J. *Orthopedics.* 1991; 14:305–308. [PubMed: 2020629]
26. Duran LW. *Med. Device Technol.* 2000; 11:14–17. [PubMed: 15326787]
27. Coester LM, Nepola JV, Allen J, Marsh JL. *Iowa Orthop J.* 2006; 26:48–53. [PubMed: 16789449]
28. Ma ML, Hill RM. *Curr. Opin. Colloid Interface Sci.* 2006; 11:193–202.
29. Hetrick EM, Shin JH, Stasko NA, Johnson CB, Wespe DA, Holmuhamedov E, Schoenfisch MH. *Acs Nano.* 2008; 2:235–246. [PubMed: 19206623]

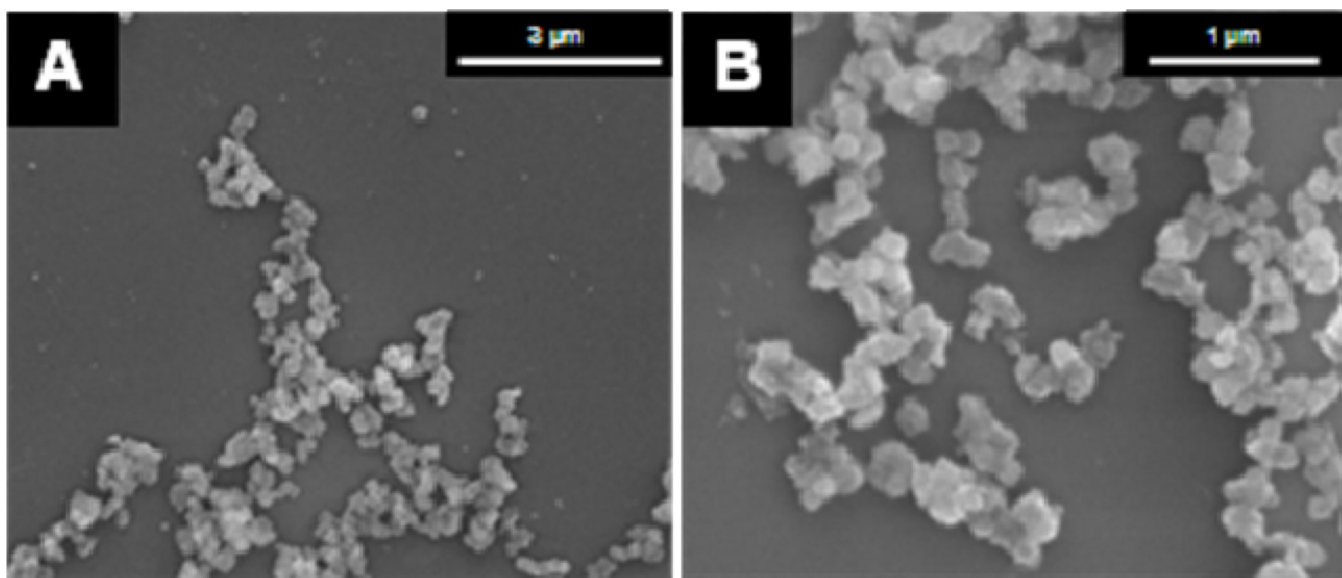


Figure 1. Scanning electron microscopy images of 30 mol% 17FTMS-TEOS silica colloids at (A) 15000 \times , and (B) 36,600 \times magnification.

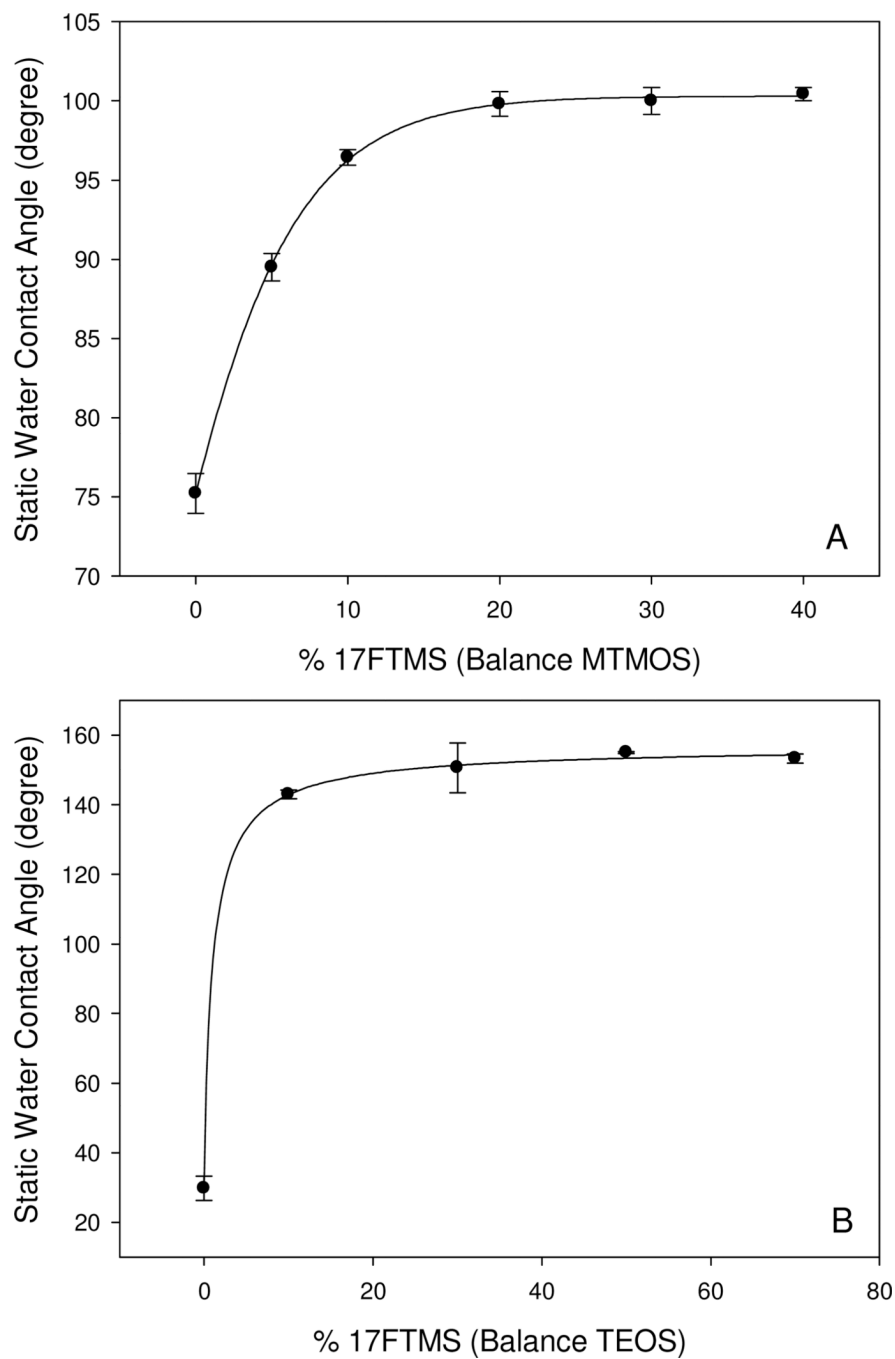


Figure 2. Static water contact angles of (A) xerogel films, and (B) silica colloids as a function of the concentration (mol%) of 17FTMS (balance MTMOS and TEOS for films and particles, respectively). Data are represented as means \pm SD ($n = 15$).

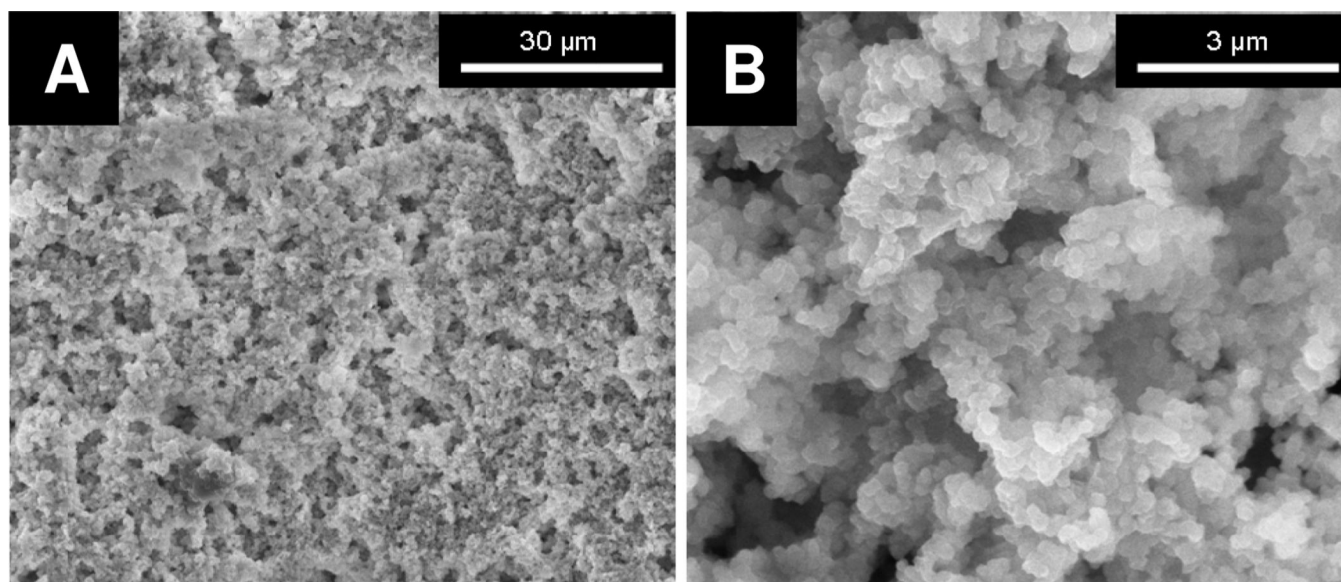


Figure 3. Scanning electron microscopy images of 30 mol% 17FTMS (balance MTMOS) xerogel films doped with 30 mol% 17FTMS (balance TEOS) silica colloids at (A) 1500 \times , and (B) 15,000 \times magnification.

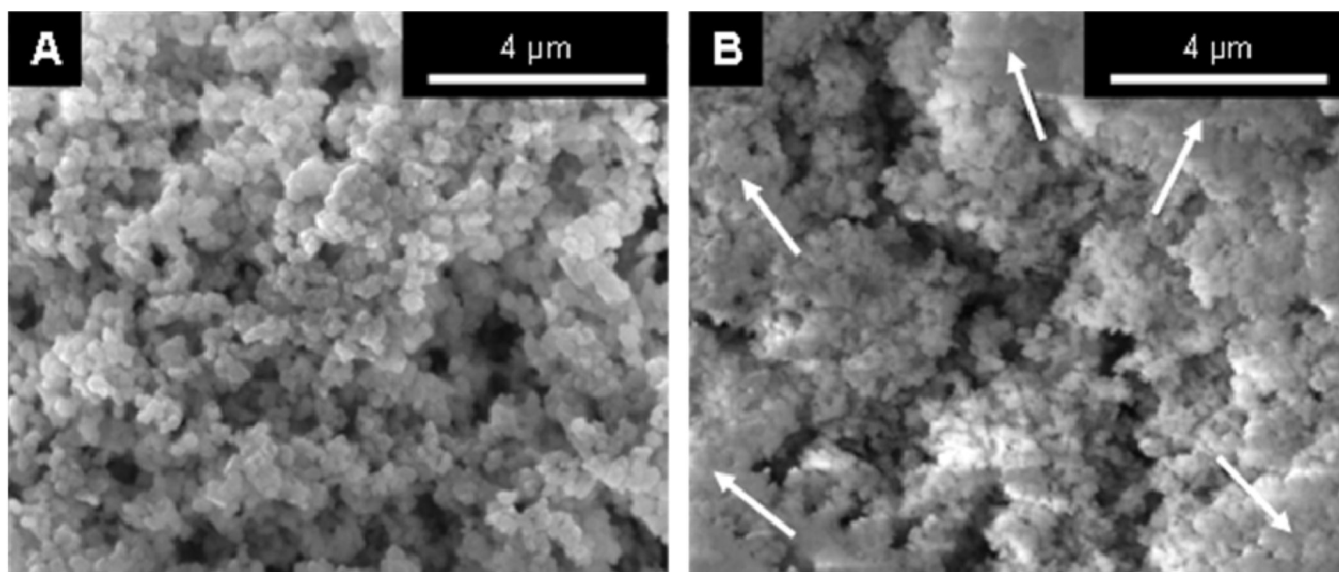


Figure 4. SEM images of A) a fluorinated xerogel (30 mol% 17FTMS-MTMOS) doped with silica colloids (30 mol% 17FTMS-TEOS) and B) a non-fluorinated xerogel (100 mol% MTMOS) doped with silica colloids (30 mol% 17FTMS-TEOS). White arrows indicate examples of smooth colloid islands.

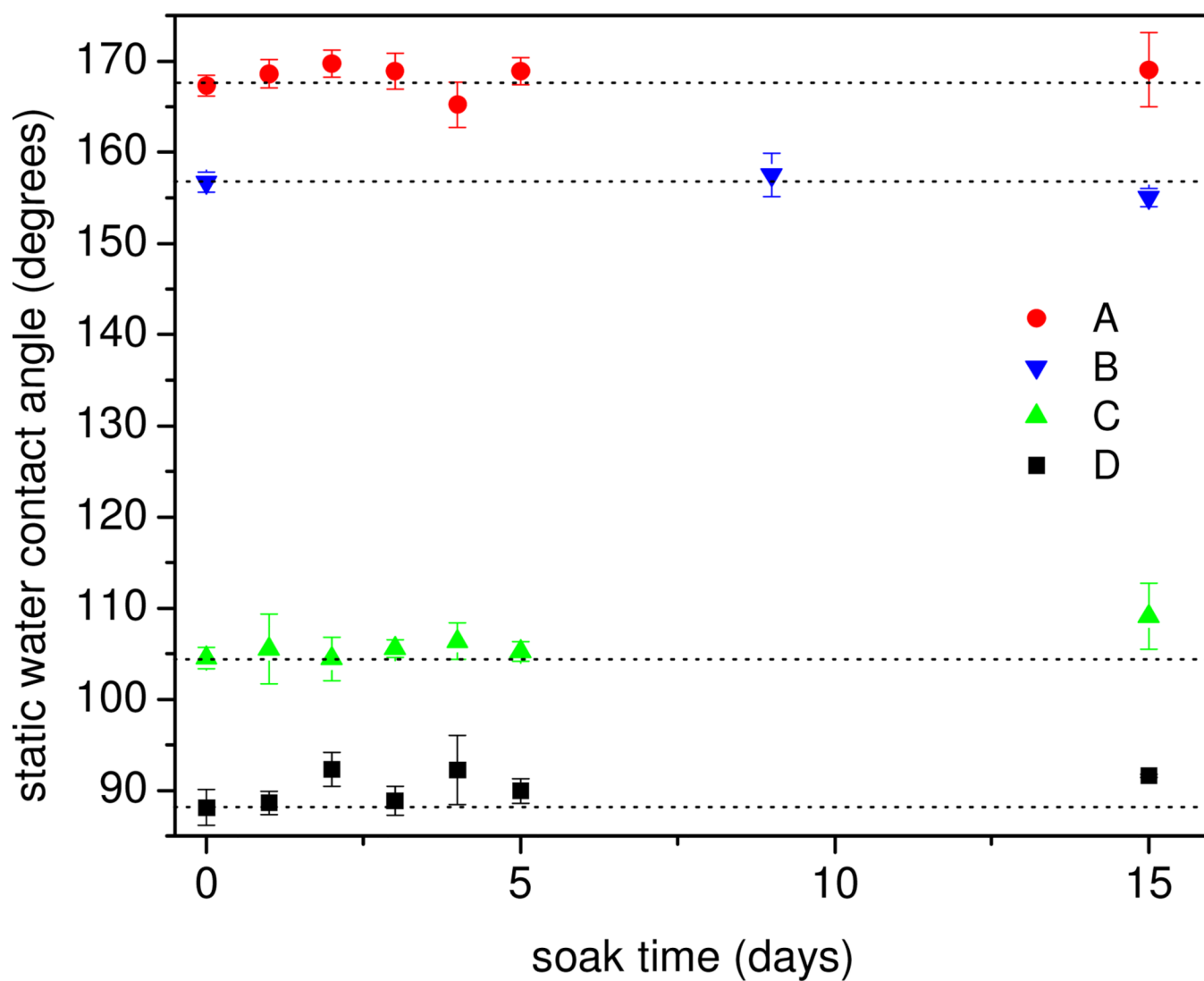


Figure 5. Static water contact angles after immersion in distilled water at 25 °C. A) Superhydrophobic 30 mol% 17FTMS (balance TEOS) colloid-doped 30 mol% 17FTMS (balance MTMOS) and B) colloid-doped 100 mol% MTMOS xerogels; C) blank (no colloids) 30 mol% 17FTMS (balance MTMOS) xerogels; and, D) MTMOS controls (100 mol%). Data are represented as means \pm SD (n = 12).

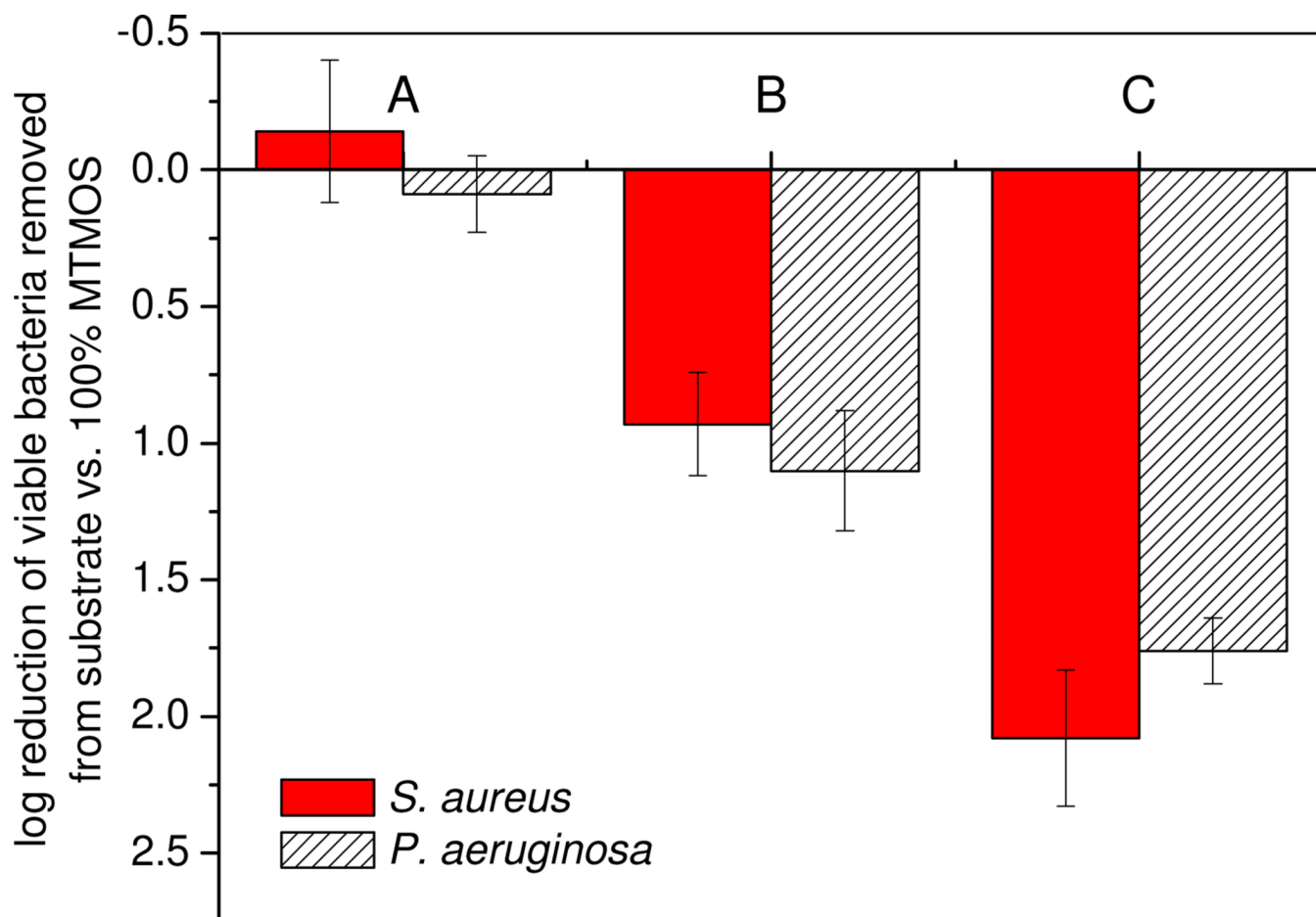
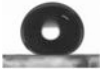





Figure 6. Reduction in *S. aureus* and *P. aeruginosa* adhesion at (A) blank (no colloids) 30 mol% 17FTMS (balance MTMOS) xerogels; (B) colloid-doped 100 mol% MTMOS xerogels; and, (C) superhydrophobic 30 mol% 17FTMS (balance TEOS) colloid-doped 30 mol% 17FTMS (balance MTMOS) xerogels versus MTMOS controls (100 mol%). Data are represented as means \pm SD (n = 9).

Table 1

Static water contact angle measurements.

Surface	Silica colloid-doped xerogel		Xerogel blanks	
	100 mol% MTMOS	30 mol% 17FTMS-MTMOS	100 mol% MTMOS	30 mol% 17FTMS-MTMOS
				
Static water contact angle (degrees)	151.0 ± 0.5	167.7 ± 1.8	88.3 ± 5.5	104.7 ± 0.8